

Research Article

Synthesis, Characterization, and Microwave-Absorbing Properties of Polypyrrole/MnFe₂O₄ Nanocomposite

Seyed Hossein Hosseini¹ and Ahmad Asadnia²

¹Department of Chemistry, Faculty of Science, Islamic Azad University, Islamshahr Branch, Tehran, Iran

²Young Researchers Club, Islamic Azad University, Central Tehran Branch, Tehran, Iran

Correspondence should be addressed to Seyed Hossein Hosseini, shhosseini@iaiu.ac.ir

Received 24 January 2012; Revised 17 March 2012; Accepted 31 March 2012

Academic Editor: Yi Du

Copyright © 2012 S. H. Hosseini and A. Asadnia. This is an open access article distributed under the Creative Commons Attribution License, which permits unrestricted use, distribution, and reproduction in any medium, provided the original work is properly cited.

Conductive polypyrrole (PPy)-manganese ferrite (MnFe₂O₄) nanocomposites with core-shell structure were synthesized by in situ polymerization in the presence of dodecyl benzene sulfonic acid (DBSA) as the surfactant and dopant and iron chloride (FeCl₃) as the oxidant. The structure and magnetic properties of manganese ferrite nanoparticles were measured by using powder X-ray diffraction (XRD) and vibrating sample magnetometer (VSM), respectively. Its morphology, microstructure, and DC conductivity of the nanocomposite were characterized by scanning electron microscopy (SEM), Fourier transform infrared spectroscopy (FTIR), and four-wire technique, respectively. The microwave-absorbing properties of the nanocomposite powders dispersing in resin acrylic coating with the coating thickness of 1.5 mm were investigated by using vector network analyzers in the frequency range of 8–12 GHz. A minimum reflection loss of –12 dB was observed at 11.3 GHz.

1. Introduction

Recently, conducting polymer composites with both electrical and ferromagnetic properties have received tremendous attention, and study on this kind of composites has become one of the most active and promising research area. What makes conducting polymer composites so attractive is their potential applications in batteries, electrochemical display devices, molecular electronics, electromagnetics shields, microwave-absorbing materials, and so forth. Polypyrrole (PPy) is one of the most promising conducting polymers due to unique properties and excellent environmental stability [1]. Conducting polymers have emerged as a new class of materials in the last three decades. Because of their high conductivity, intriguing electrical properties, and ease of production, potential applications such as microwave absorbers were seriously considered soon after the discovery of these materials [2]. It is well known that conducting polymers can effectively shield electromagnetic waves generated from an electric source, whereas electromagnetic waves from a magnetic source can be effectively shielded only by magnetic materials. Thus, the incorporation of

magnetic constituents and conducting polymeric materials into multifunctional composites opens new possibilities for the achievement of good shielding effectiveness for various electromagnetic sources [3]. The development of microwave-absorbing materials continues to attract much attention. Among the candidates for such application, ferrites present an interesting material. The use of ferrite-based absorbers requires better performance at higher frequencies such as X-band [4].

Spinel-type ferrites have been used as conventional microwave absorption materials. However, spinel-type ferrites show Snoek's limit, and the magnetic loss decreases drastically at several gigahertz [5]. Electromagnetic wave absorbing materials used in gigahertz (GHz) range have attracted much attention with the development of GHz microwave communication, radar detection, and other industrial applications in recent years. These absorbing materials can be manufactured by a number of magnetic and dielectric materials in powder form, loaded in various kinds of polymeric binders. Various electromagnetic wave absorbing materials can be designed by using the dispersion characteristic of the complex permittivity and permeability.

Ferrite is one of materials as electromagnetic-wave-absorber, and a number of investigations have been reported for studying the effect of composition on electromagnetic wave absorption properties [6]. In the past decades, the spinel ferrites have been utilized as the most frequent absorbing materials in various forms. Manganese ferrite (MnFe_2O_4) is a common spinel ferrite material and has been widely used in microwave and magnetic recording applications. Recently, it has been shown that magnetic nanocomposites are useful as microwave-absorbing materials due to their advantages in respect to light weight, low cost, design flexibility, and microwave properties over pure ferrites [7]. The previous work, PANi-manganese ferrite nanocomposite with the magnetic behavior, is successfully synthesized by in situ polymerization of aniline in the presence of MnFe_2O_4 nanoparticles [8]. A minimum reflection loss of -15.3 dB was observed at 10.4 GHz. In this work, minimum reflection loss of -12 dB was observed at 11.3 GHz.

2. Experimental

2.1. Materials and Instrumentals. Chemicals including metal salts, hexamethylenetetramine (HMTA), potassium persulfate (KPS), and ethylene glycol (EG) are analytical grade (Merck) and were used without further purification. Water was deionized, doubly distilled, and deoxygenated prior to use. Styrene and methacrylic acid (analytical grade, Merck) were distilled to remove the inhibitor. Pyrrole monomer (analytical grade, Merck) was distilled twice under reduced pressure. DBSA and acrylic resin were of industrial grade. The other reagent, including iron chloride (FeCl_3), was of analytical grade (Merck).

The morphology of coated particles and nanocomposite was observed by scanning electron microscopy (SEM) with a JSM-6301F (Japan) instrument operated at an accelerating voltage of 10 kV. X-ray powder diffraction (XRD) patterns of the nanoparticles assemblies were collected on a Philips-PW 1800 with Cu-K radiation under $\text{CuK}\alpha$ radiation ($\lambda = 1.5406 \text{ \AA}$). Fourier transform infrared spectroscopy (FTIR) spectra were recorded on a PerkinElmer spectrum FTIR using KBr pellets. The M-H hysteresis loops were measured by vibrating sample magnetometer (VSM) (RIKEN DENSHI Co. Ltd., Japan). Microwave-absorbing properties were measured by vector network analyzers (Agilent Technologies Inc. 8722) in the 8–12 GHz range at room temperature.

2.2. Preparation of Nanoparticles (see [9])

2.2.1. PS Colloid. Negatively charged PS spheres with average diameter 230 nm, which were used as core particles, were prepared by a free-emulsion polymerization method [10]. In a typical experiment, 10 mL styrene, 2 mL methacrylic acid, and 0.054 g KPS were added to the flask with 100 mL deionized water. To eliminate oxygen effects, the solution was purged with nitrogen before the process was initiated. The mixture was heated to 72°C and stirred with a magnetic stirrer. The polymerization was continued for 24 h, and in the whole procedure the nitrogen was purged. Concentration

of PS spheres in solution is 80 mg/mL, which was calculated by drying 5 mL colloid solution and weighing the remained solids.

2.3. Coated Particles. The coating procedure consisted of controlled hydrolysis of aqueous solutions of ferrous chloride and other divalent metal salts in the presence of polystyrene latexes. In a typical preparation process, 2 mL PS colloid solution was diluted with 250 mL deoxygenated distilled water and then mixed with the metal salts solution, which contained 10 mmol FeCl_2 and 5 mmol MnCl_2 . After dispersed under ultrasonic for several minutes, the mixture was incorporated with 4 g HMTA and 0.5 g potassium nitrate and heated to 85°C under gentle stirring. After 3 h, the system was cooled to room temperature. The solution was poured into excess distilled water, then magnetic particles were deposited using magnetic field. The precipitate was washed with distilled water for several times and then dried in oven at 80°C for 24 h. In addition, to modify the surface chemical properties of the composites magnetic spheres, 5 mL ethylene glycol (EG) was added into the reaction solution before the incorporation of HMTA.

2.4. Synthesis of MnFe_2O_4 -PPy Nanocomposite with Core-Shell Structure. MnFe_2O_4 -PPy core-shell nanocomposites were prepared by in situ polymerization in the presence of DBSA as the surfactant and dopant and FeCl_3 as the oxidant. The DBSA was dissolved in distilled water with vigorous stirring for about 20 min, then MnFe_2O_4 nanoparticles (0.73 g) were added to the DBSA solution under stirring for approximately 1 h. Then 5 mL of pyrrole monomer was added to the suspension and stirred for 30 min. MnFe_2O_4 nanoparticles were dispersed well in the mixture of pyrrole/DBSA under ultrasonication for 2 h. 23.5 g FeCl_3 in 60 mL deionized water was slowly added dropwise to the mixture with a constant stirring. The polymerization with stirring under an ice-water bath was allowed to proceed for 4 h. The nanocomposite was obtained by filtering and washing the suspension with deionized water and ethanol, respectively. The obtained black powder with the content of 15 wt% MnFe_2O_4 was dried under vacuum for 24 h.

3. Results and Discussion

3.1. X-Ray Diffraction. Figure 1 shows the XRD pattern of manganese ferrites. It can be clearly noted from Figure 1 that the ferrite shell are phase-pure spinel structure in all cases according to the standard XRD patterns of the spinel ferrite Fe_3O_4 ($2\theta = 30.1, 35.5, 43.7, 53.2, 57.0, 62.4, 74.0, 78.0$) Mn ferrite ($2\theta = 33.0, 71.0, 86.5$), and NaCl ($2\theta = 75.4$). The average crystallite size was calculated using software Originpro75 through the diffraction speaks from Scherer's formula as shown below:

$$D = 0.89 \frac{\lambda}{\beta} \cos \theta, \quad (1)$$

where D is the crystal size, λ is the X-ray wavelength, β is the broadening of the diffraction peak, and θ is the diffraction

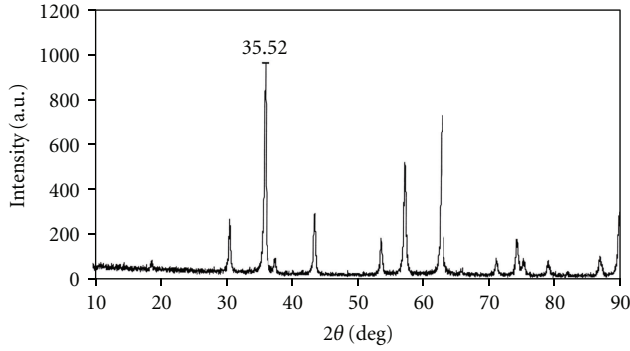


FIGURE 1: X-ray diffraction for MnFe_2O_4 .

angle. Calculated by the Scherrer formulation, the mean crystallite size of the ferrite particles is 24.27 nm.

3.2. Magnetic Properties. Figures 2(a) and 2(b) show the magnetization (M) versus the applied magnetic field (H) for MnFe_2O_4 and $\text{MnFe}_2\text{O}_4/\text{PPy}$ nanocomposite (15 wt%) respectively. The magnetic properties of the ferrite-coated PS latex were analyzed by room temperature VSM with an applied field $-10 \text{ kOe} \leq H \leq 10 \text{ kOe}$. It can be inferred from the hysteresis loops that all the composite magnetic spheres are magnetically soft at room temperature. The value of saturation magnetization (M_s) is about 66.7 emu/g, the remnant magnetization (M_r), and coercivity field are 17.81 emu/g and 110 Oe, respectively. Figure 2(b) shows clear saturation $-10 \leq H \leq 10 \text{ kOe}$ with saturation magnetization (M_s) about 10 emu/g and the remnant magnetization (M_r) about 3.4 emu/g, for nanocomposite which is lower than pure manganese ferrite nanoparticles, so the magnetization curve of the sample shows weak ferromagnetic behavior, with slender hysteresis. Magnetic properties of nanocomposites containing magnetite or ferrite particles have been believed to be highly dependent on the sample shape, crystallinity, and the value of magnetic particles, so that they can be adjusted to obtain optimum property. Magnetic properties of nanocomposite and ferrite particles showed soft magnetization behavior.

3.3. Morphology Investigation. Figures 3(a), 3(b), and 3(c) show the SEM images for the MnFe_2O_4 and $\text{MnFe}_2\text{O}_4/\text{PPy}$ nanocomposite, respectively. As shown in Figure 3(a), the spongy-shaped MnFe_2O_4 was seen with a small quantity of amorphous phase. The length of spongy-shaped MnFe_2O_4 average diameter is about 80–90 nm. In Figures 3(b) and 3(c), it is found that the $\text{MnFe}_2\text{O}_4/\text{PPy}$ nanocomposite (15 wt%) still retains the morphology of PPy shape. It is much unknown how to form spongy-shaped composite in the polymerization process. The SEM image clearly shows that the MnFe_2O_4 was distributed rather homogeneously and ultrasonication is effective for dispersing nanoferrite in the polymer matrix.

The length of $\text{MnFe}_2\text{O}_4/\text{PPy}$ nanocomposite average diameter is about 60–130 nm.

3.4. FTIR Spectra. Figures 4(a) and 4(b) show FTIR spectra of MnFe_2O_4 and $\text{PPy-MnFe}_2\text{O}_4$ nanocomposite, respectively. In ferrites, the metal ions are usually situated in two different sublattices, designated as tetrahedral and octahedral sites according to the geometrical configuration of the oxygen nearest neighbors [9]. It was observed from Figure 4(a) that the peak at 570.22 cm^{-1} is intrinsic vibrations of manganese ferrite. The characteristic peaks of styrene occur at 1638, 1458.04, 1008.65–1382.16, 811.30 and 865.50 cm^{-1} . The peak at 1638 is attributed to the styrene ring. The peak at 1458 cm^{-1} is attributed to the characteristic C=C stretching ring. The peaks at 811.30, and 865.50 cm^{-1} are related to the C–H outer bending vibrations.

As shown in Figure 4(b), the characteristic peaks of PPy-manganese ferrite nanocomposite occur at 2920, 1555, 1461, 1313, 1188, 1038, 1006, 959, 908, 670, and 576 cm^{-1} . The peaks at 1555 and 1461 cm^{-1} are attributed to the characteristic C=C and C–N stretching of polypyrrole ring; the peaks at 1313 and 1188 cm^{-1} correspond to N–H bending and asymmetric C–N stretching modes of the PPy ring, respectively. The peak around 1038 cm^{-1} is associated with vibrational modes of N=Q=N (Q refers to the quinonic type rings), indicating that PPy is formed in our sample. The peaks at 2920 and 1038 cm^{-1} attributed to C–H aliphatic stretching vibration and the symmetric and antisymmetric stretching vibration of SO_3 group of dopant (DBSA), respectively. The peaks at $1006\text{--}908 \text{ cm}^{-1}$ are attributed to the *p*-disubstituted aromatic ring C–H out-of-plane bending. However, the characteristic peaks of MnFe_2O_4 for F–O and Mn–O stretching vibrations can be observed at wave numbers 670 and 576 cm^{-1} .

3.5. Microwave-Absorbing Properties. According to transmission line theory, the reflection loss (RL) of electromagnetic radiation, under normal wave incidence at the surface of a single-layer material backed by a perfect conductor can be given by

$$\text{RL} = 20 \log \left| \frac{Z_{in} - Z_0}{Z_{in} + Z_0} \right|, \quad (2)$$

where Z_0 is the characteristic impedance of free space:

$$Z_0 = \sqrt{\frac{\mu_0}{\epsilon_0}}. \quad (3)$$

Z_{in} is the input impedance at free space and materials interface:

$$Z_{in} = \sqrt{\frac{\mu_r}{\epsilon_r} \tanh \left[j \frac{2\pi f t}{c} \sqrt{\mu_r \epsilon_r} \right]}, \quad (4)$$

where μ_r and ϵ_r are the complex permeability and permittivity of the composite medium, respectively, which can be calculated from the complex scatter parameters, c is the light velocity, f is the frequency of the incidence electromagnetic wave, and t is the thickness of composites. The impedance-matching condition is given by $Z_{in} = Z_0$ to represent the perfect absorbing properties [9]. There are two

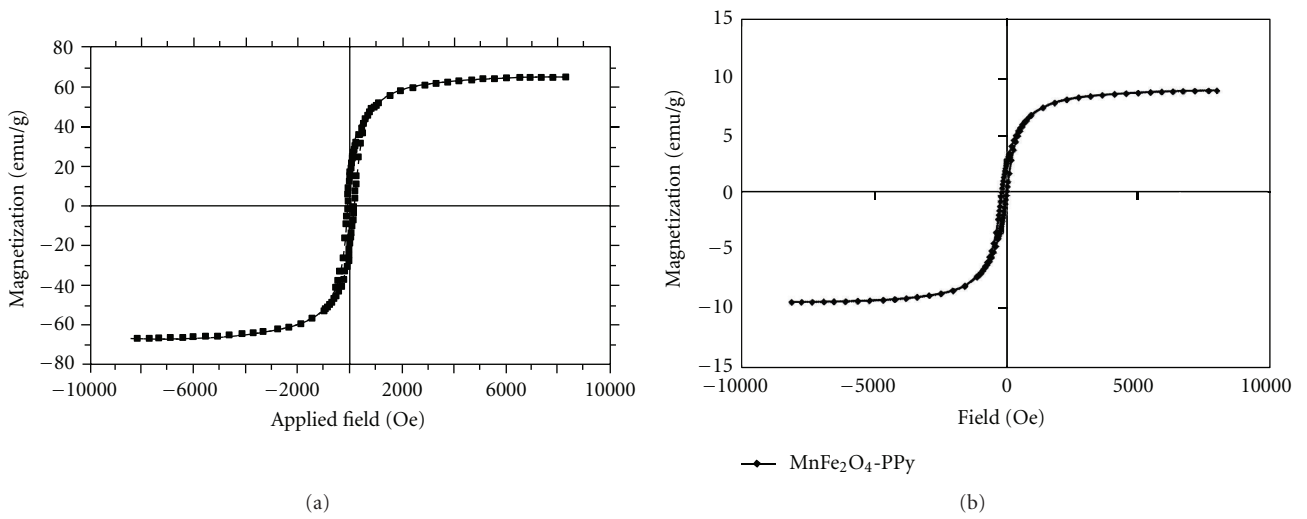


FIGURE 2: Magnetic hysteresis loop of (a) MnFe₂O₄ nanoparticle and (b) MnFe₂O₄/PPy nanocomposite.

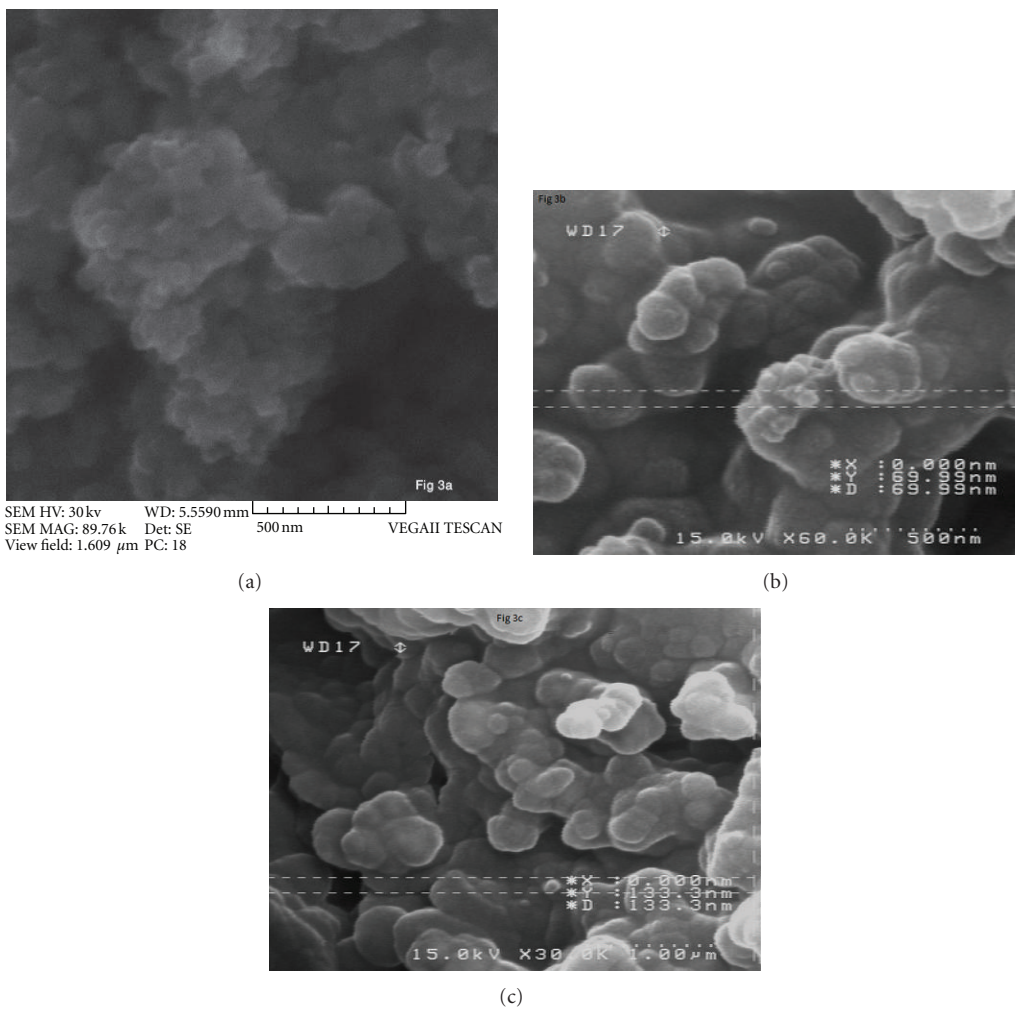


FIGURE 3: SEM microphotographs of (a) MnFe₂O₄ nanoparticle and ((b), (c)) MnFe₂O₄/PPy nanocomposite.

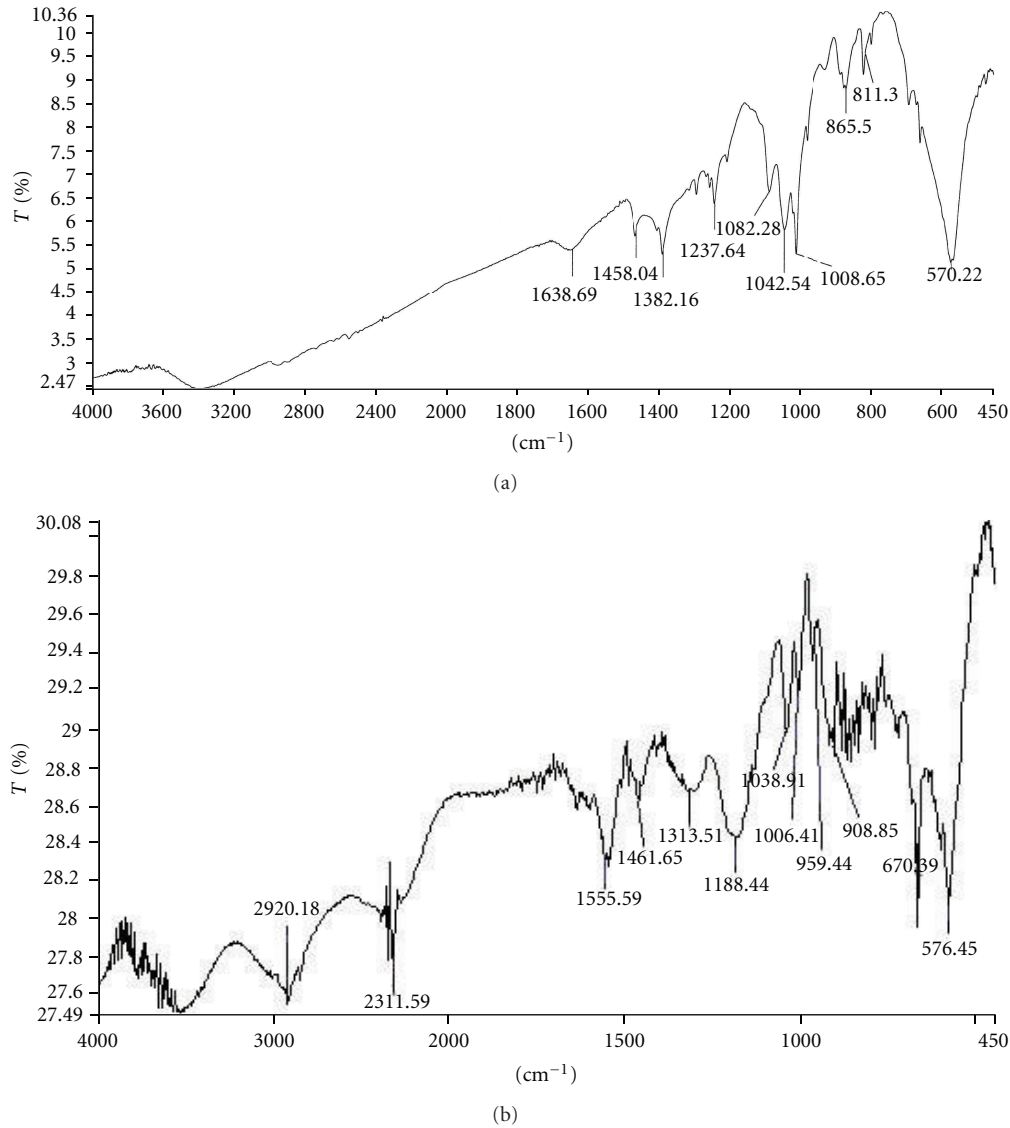


FIGURE 4: FTIR spectra: (a) MnFe_2O_4 nanoparticle and (b) $\text{MnFe}_2\text{O}_4/\text{PPy}$ nanocomposite.

different concepts to satisfy the zero-reflection condition. The first concept is the “matched characteristic impedance.” The intrinsic impedance characteristic of material is made equal to the impedance characteristic of the free space. The second is the “matched-wave-impedance” concept. The wave impedance at the surface of the metal-backed material layer is made equal to the intrinsic impedance of the free space. In this work, the second concept was applied. The condition of maximal absorption is satisfied at a particular point where thickness and frequency match each other. Ferrites are the only materials that present two matching frequencies and thicknesses. The first matching at low frequency is associated with the mechanisms of magnetic resonance and shows a dependence on the chemical composition. The second matching at high frequency is associated with the thickness of absorber material. To satisfy the zero-reflection condition where maximum absorption would occur, Z_{in} should be 1

to prevent reflection. This can be ideally achieved when the material presents $|\mu_r| = |\epsilon_r|$. In this case, the performance of electromagnetic wave-absorbing material increases linearly with the increase in thickness. In practical terms, however, this is rarely achieved because the values of complex permeability and complex permittivity are very different in the frequency range of interest. When $|\mu_r| \neq |\epsilon_r|$, we should consider two other cases. For materials with intrinsic impedances greater than unity, $|\mu_r| > |\epsilon_r|$, the minimum reflection loss occurs at around a half-wavelength thickness of the material, and for materials with intrinsic impedances lower than unity, $|\mu_r| < |\epsilon_r|$, the minimum reflection loss occurs at around a quarter-wavelength thickness of the material. Within the microwave region, ferrites usually present electromagnetic characteristics of $|\mu_r| < |\epsilon_r|$, giving rise to the term “quarter-wavelength absorbers.” Minimum loss occurs when the thickness is about an odd multiple

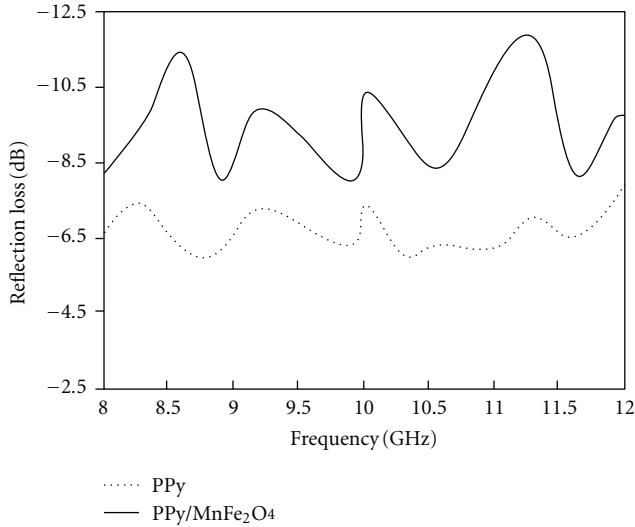


FIGURE 5: Frequency dependence of RL for the $\text{MnFe}_2\text{O}_4/\text{PPy}$ nanocomposite.

of one quarter of the wavelength of the incident frequency, measured inside the absorbing material, and the material has the proper loss factor for this particular thickness. The thickness, d , can be written as (5), where c is the speed of light and f is the frequency of interest [11]:

$$d = \frac{c}{4f\sqrt{|\mu_r||\epsilon_r|}}. \quad (5)$$

Nanocomposite powders dispersed in acrylic resins, then the mixture was pasted on metal plate with the area of $100\text{ mm} \times 100\text{ mm}$ as the test plate. The microwave-absorbing properties of the nanocomposite with the coating thickness of 1.5 mm, were investigated by using vector network analyzers in the frequency range of 8–12 GHz. Figure 5 shows the variation of reflection loss versus frequency determined from PPy-manganese ferrite nanocomposite. For MnFe_2O_4 composites with the coating thickness of 1.5 mm, the reflection loss values less than -12 dB were obtained in the frequency of 8–12 GHz and its value of minimum reflection loss is -12 dB at the frequency of 11.3 GHz.

4. Conclusion

The obtained magnetic nanoparticles are of a diameter of 24.27 nm. PPy-manganese ferrite nanocomposite with the magnetic behavior is successfully synthesized by in situ polymerization of pyrrole in the presence of MnFe_2O_4 nanoparticles. The results of spectroanalysis indicate that there is an interaction between PPy chains and ferrite particles. A minimum reflection loss of -12 dB was observed at 11.3 GHz with at thickness of 1.5 mm of nanocomposite.

References

- [1] C. Zhang, Q. Li, and Y. Ye, "Preparation and characterization of polypyrrole/nano- $\text{SrFe}_{12}\text{O}_{19}$ composites by in situ polymerization method," *Synthetic Metals*, vol. 159, no. 11, pp. 1008–1013, 2009.
- [2] V. T. Truong, S. Z. Riddell, and R. F. Muscat, "Polypyrrole based microwave absorbers," *Journal of Materials Science*, vol. 33, no. 20, pp. 4971–4976, 1998.
- [3] B. Birsöz, A. Baykal, H. Sözeri, and M. S. Toprak, "Synthesis and characterization of polypyrrole- $\text{BaFe}_{12}\text{O}_{19}$ nanocomposite," *Journal of Alloys and Compounds*, vol. 493, no. 1-2, pp. 481–485, 2010.
- [4] T. Giannakopoulou, L. Kompotiatis, A. Kontogeorgakos, and G. Kordas, "Microwave behavior of ferrites prepared via sol-gel method," *Journal of Magnetism and Magnetic Materials*, vol. 246, no. 3, pp. 360–365, 2002.
- [5] S. Sugimoto, K. Haga, T. Kagotani, and K. Inomata, "Microwave absorption properties of Ba M-type ferrite prepared by a modified coprecipitation method," *Journal of Magnetism and Magnetic Materials*, vol. 290-291, pp. 1188–1191, 2005.
- [6] F. Tabatabaie, M. H. Fathi, A. Saatchi, and A. Ghasemi, "Microwave absorption properties of Mn- and Ti-doped strontium hexaferrite," *Journal of Alloys and Compounds*, vol. 470, no. 1-2, pp. 332–335, 2009.
- [7] H. M. Xiao, X. M. Liu, and S. Y. Fu, "Synthesis, magnetic and microwave absorbing properties of core-shell structured $\text{MnFe}_2\text{O}_4/\text{TiO}_2$ nanocomposites," *Composites Science and Technology*, vol. 66, no. 13, pp. 2003–2008, 2006.
- [8] S. H. Hosseini, S. H. Mohseni, A. Asadnia, and H. Kerdari, "Synthesis and microwave absorbing properties of polyaniline/ MnFe_2O_4 nanocomposite," *Journal of Alloys and Compounds*, vol. 509, no. 14, pp. 4682–4687, 2011.
- [9] Y. Zhang, Z. Huang, F. Tang, and J. Ren, "Ferrite hollow spheres with tunable magnetic properties," *Thin Solid Films*, vol. 515, no. 4, pp. 2555–2561, 2006.
- [10] G. Mu, N. Chen, X. Pan, H. Shen, and M. Gu, "Preparation and microwave absorption properties of barium ferrite nanorods," *Materials Letters*, vol. 62, no. 6-7, pp. 840–842, 2008.
- [11] A. R. Bueno, M. L. Gregori, and M. C. S. Nóbrega, "Microwave-absorbing properties of $\text{Ni}_{0.50-x}\text{Zn}_{0.50-x}\text{Me}_{2x}\text{Fe}_2\text{O}_4$ (Me 1/4 Cu, Mn, Mg) ferrite wax composite in X-band frequencies," *Journal of Magnetism and Magnetic Materials*, vol. 320, no. 6, pp. 864–870, 2008.



Hindawi

Submit your manuscripts at
<http://www.hindawi.com>

